Research Article Vol. 13, No. 4 / 1 Apr 2022 / Biomedical Optics Express 1899
Biomedical Optics EXPRESS

Femtosecond Er-doped fiber laser source tunable from 872 to 1075 nm for two-photon vision studies in humans

DOROTA STACHOWIAK,[1,*] MARCIN MARZEJON,[2,3] JAKUB BOGUSŁAWSKI,[1,2,4] ZBIGNIEW ŁASZCZYCH,[1] KATARZYNA KOMAR,[2,4,5] MACIEJ WOJTKOWSKI,[2,4] AND GRZEGORZ SOBOŃ[1]

[1]*Laser & Fiber Electronics Group, Faculty of Electronics, Photonics and Microsystems, Wrocław University of Science and Technology, Wybrzeże Wyspiańskiego 27, 50-370 Wrocław, Poland*
[2]*Department of Physical Chemistry of Biological Systems, Institute of Physical Chemistry, Polish Academy of Sciences, Kasprzaka 44/52, 01-224 Warsaw, Poland*
[3]*Department of Metrology and Optoelectronics, Faculty of Electronics, Telecommunications and Informatics, Gdańsk University of Technology, G. Narutowicza 11/12, 80-233 Gdańsk, Poland*
[4]*International Centre for Translational Eye Research, Skierniewicka 10a, 01-230 Warszawa, Poland*
[5]*Institute of Physics, Faculty of Physics, Astronomy and Informatics, Nicolaus Copernicus University in Torun, Grudziądzka 5, 87-100 Toruń, Poland*
[*]*dorota.stachowiak@pwr.edu.pl*

Abstract: We report the development of a widely-tunable femtosecond fiber laser system and its application for two-photon vision studies. The source is based on an Er-doped fiber laser with spectral shift up to 2150 nm, followed by a second harmonic generation module to generate a frequency-doubled beam tunable from 872 to 1075 nm. The source delivers sub-230 fs pulses with nearly-constant duration over the entire tuning range, with output powers between 0.68–1.24 mW, which corresponds to a pulse energy of 13.2–24.1 pJ. Such pulse energy is sufficient for employing a system for measurements of two-photon scotopic spectral sensitivity of two-photon vision in humans. The laser parameters allow for very efficient and safe two-photon stimulation of the human visual system, as proved by a good separation between one- and two-photon thresholds for wavelengths below 950 nm, which we have confirmed for 3 healthy subjects.

1. Introduction

Spectrally tunable femtosecond laser sources are suitable tools for many biomedical applications, including pharmacology, multiphoton microscopy, optical imaging, and non-invasive diagnostics [1–3]. One of the experimental techniques of the latter group is two-photon microperimetry (2PM) [4]. It is a novel method of visual field examination, based on the two-photon vision (2PV) phenomenon, in which a pulsed infrared light source is perceived due to two-photon absorption occurring in visual pigments [5]. The 2PV extends the visible region of electromagnetic radiation, enabling humans to perceive wavelengths of 800–1200 nm of having colors as 400–600 nm, their half-wavelength counterparts [6,7]. Palczewska et al. demonstrated that two-photon vision occurs over the spectral range of 950-1200 nm for laser of repetition rate 76 MHz and pulses of duration of single picoseconds [5]. The impact of pulse train parameters for 2PV was further analyzed by Marzejon et al.: it was shown that the 2PV threshold depends on the integral of the squared instantaneous power [8]. Thus, pulse lengthening to tens of picoseconds could be compensated by reducing the laser repetition rate. Indeed, Manzanera et al. used a source with pulses on the order of 1 ns, with repetition rates of 1.98 kHz and 9.91 kHz for 2PV experiments [9]. However, increasing the duty cycle of the laser causes a decrease of 2PV visibility until the visual threshold approaches the limit set by safety standards [10]. Therefore, the practical applications of lasers with long pulses and low repetition rates for 2PV studies are limited.

#452609 https://doi.org/10.1364/BOE.452609
Journal © 2022 Received 3 Jan 2022; revised 16 Feb 2022; accepted 24 Feb 2022; published 4 Mar 2022

Biomedical Optics EXPRESS

The potential advantages of 2PV arise from the fundamental differences compared to normal, single-photon vision. The infrared radiation could be beneficial for sensitivity testing in case of cataract or other age-related opacifications because it is less scattered and absorbed than the radiation of a shorter wavelength [4,11]. The brightness of light perceived due to the 2PV depends on the square of intensity (power per unit area) [4,12]. This feature entails a narrower psychometric function compared to normal vision because the seen-unseen boundary covers a narrower range of intensities [4]. Therefore visual threshold can be determined with better precision which is particularly advantageous to microperimetric testing. The two-photon absorption is limited only to the focal region of the laser beam and unfocused, scattered light is not perceived due to 2PV. The resulting advantage for ophthalmology and vision science applications is the greater precision of retinal stimulation than for normal single-photon vision. It may be also beneficial for virtual/augmented reality applications.

In contrary to single-photon vision, there is no exact and comprehensive information on spectral dependence of two-photon visual thresholds. So far, there are only three published sets of data on this subject, obtained with a limited number of participants: 2–4. Historically the first one was published by Dmitriev et al. in 1979 [13]. The paper shows a two-photon sensitivity curve in the range of 1000–1150 nm: it has a complex structure containing several narrow bands superimposed on a wider envelope with a maximum of 1113 ± 15 nm. Such complex structure was not confirmed in more recent studies: Palczewska et al. [5] and Manzanera et al. [9]; however, the ranges and density of measurement points were different than in Dmitriev's paper. Measurements reported by Palczewska et al. were performed in the 750–1080 nm range in 25–50 nm increments and with only one point at 1150 nm. Manzanera et al. showed results from 850–1100 nm with similar intervals to that obtained by Palczewska et al. According to Manzanera et al., the two-photon sensitivity in 1000–1100 nm seems to be rather flat, and Palczewska et al. show that position of maximum is strongly dependent on the pulse duration. Thus comparison of results discussed above is impeded by the fact that each sensitivity curve was acquired with a laser source of different pulse duration and repetition rate, both of which affect the two-photon visual threshold [8]. The lack of unambiguous data on the sensitivity curve of 2PV significantly hinders both the study of this process and the development of methods based on it. The 2PM is still in the early development stage, and its applicability to diagnostics of ocular pathology or treatment monitoring is still being examined [14,15]. Also, the requirements for the parameters of the apparatus used for the 2PM are constantly under development [8,16]. The femtosecond Yb-doped lasers (both fiber-based and solid-state) available on the market and used in state-of-the-art microperimetry are very well-established devices with excellent optical properties [4,8]. Nevertheless, they have one main drawback, limiting their application in 2PV studies: a fixed emission wavelength (located around 1030 nm). Due to this limitation, 2PM allows only measuring the subject's ability to perceive ~1 μm infrared light as green. Extending the wavelength range could provide an opportunity to selectively stimulate different photoreceptors since the one-photon absorption spectra of rod and cones' photopigments are different [17], and their two-photon absorption spectra can be expected to differ as well. The more selective stimulation of photoreceptors as a potential specific factor for diagnosing and monitoring human eye diseases could also be beneficial for 2PM. Summarizing, using a single laser source, with possible wavelength tuning and constant pulse duration and pulse repetition rate in the whole spectral range of interest, with parameters meeting the eye safety norms, would allow for comprehensive studies of the 2PV phenomenon.

Nevertheless, achieving wide spectral tuning in the entire 2PV range is challenging since there are no direct methods enabling such broad femtosecond emission from any known gain medium. A most common choice for two-photon microscopy is a Ti:Sapphire laser, which offers wavelength tunability from approx. 700 to 1080 nm with ultrashort pulse duration. However, Ti:Sapphire is a quite complex and expensive device, as it needs a high-power green solid-state laser for

Biomedical Optics EXPRESS

pumping. Typically, such lasers also require periodic maintenance, translating into the high cost of ownership. While considering a future clinical translation of two-photon microperimetry, the implementation potential of Ti:Sapphire lasers and associated high-upkeep instrumentation is relatively low. A Ti:Sapphire requires an optical table for installation and separate units for driving electronics and a chiller. Its another fundamental limitation is in setting the value of the repetition rate arising from a fixed cavity length that cannot be easily changed. Control of the pulse parameters is thus limited. It is possible to use a pulse picker, but this approach usually increases the size and cost of the device, and introduces extra dispersion. Controlling the repetition rate with a pulse picker in a fiber laser is much simpler, as we have shown in our previous studies [18]. From this perspective, a compact, maintenance-free fiber laser could be an interesting alternative when watt-level output power is not required.

The spectral range of interest of 2PV studies might be addressed with the use of novel fiber-based technology and nonlinear optics. One can use a femtosecond laser at 1.55 μm wavelength, convert its output to a longer wavelength (1.8–2.1 μm) utilizing the soliton self-frequency shift effect (SSFS) [19–21], and finally frequency-double it in the second harmonic generation (SHG) process [22–24]. An example of such a solution was presented by Li et al. in [25]. A pulsed laser source operating at 1550 nm was used for SSFS in a large mode area (LMA) fiber, allowing it to reach the wavelength of 2500 nm. As a result of the SHG process, tuning in the wavelength range from 950 to 1260 nm was achieved, with the pulse duration varying between 76 and 180 fs. The main challenge in such a setup was the presence of multiple higher-order solitons generated in the SSFS process. Another approach was presented by Chou et al. in [26], where femtosecond pulses at 1025 nm were launched into a photonic crystal fiber to induce spectral broadening up to 740–1236 nm via strong self-phase modulation (SPM) phenomenon. The pulse duration in the entire range was measured to be below 100 fs. However, the achieved wavelength tuning range had a large gap between 914 and 1135 nm (over 200 nm) resulting from using the Yb-laser as a pump source. A different approach was presented in [27], where a three-color femtosecond laser source was developed. The system was operating at three wavelengths: 775 nm (generated from the SHG of the 1550 nm femtosecond laser source), 864 nm, and 950 nm (generated from 1728 nm and 1900 nm solitons generated through SSFS in the LMA fiber) and delivered pulses with durations of 245 fs, 132 fs, and 88 fs, respectively. Krauss et al. [28] have presented a combination of two methods. A mode-locked Er-doped fiber laser was used as a seed for two parallel amplifier stages with a silicon prism compressor at their outputs. The compressed signal from one of the amplifiers was directly frequency-doubled, providing a signal at 775 nm wavelength with the 1 ps pulse duration (2.4 nJ of pulse energy). The compressed output from the second amplifier was delivered into a nonlinear fiber, where the solitons were shifted to longer wavelengths and frequency-doubled, providing wavelength tuning in the range of 850–1100 nm. All these sources were successfully applied in potential biomedical applications, such as in vivo two-photon fluorescence microscopy [25], simultaneous two-color two-photon fluorescence microscopy of endogenous fluorophores [26], two-photon microscopy of human melanoma cells [27], and coherent anti-Stokes Raman scattering spectroscopy [28]. However, there are still drawbacks which need to be overcome, like the gap in the tuning range or inconstant pulse duration for the entire tuning bandwidth.

In this work, we report a new design of a frequency-doubled spectrally shifted Er-doped fiber laser tailored to the needs of eye diagnostics applications such as 2PV-based visual field testing. The developed system delivers stable sub-230 fs pulses in a broad wavelength tuning range of over 200 nm (872.1–1074.9 nm). This allows for reliable experiments to obtain the scotopic luminosity curve for 2PV in this spectral range, eliminating laser-dependent factors influencing the measurement reliability. The laser tuning range covers the region where two-photon vision becomes dominant over single-photon vision (900-1000 nm), which is important for future studies. Furthermore, the laser may be used for two-photon stimulation of S-cones with 950 nm wavelength

Biomedical Optics EXPRESS

as proved by blue color perception without the addition of red. The wide wavelength tuning range, compactness, stable average power at each wavelength, and nearly constant pulse duration over the entire tuning range make the source an attractive alternative for, e.g., commercially available ytterbium-doped fiber laser emitting pulses at the 1030 nm wavelength.

2. Experimental setup of the spectrally-shifted frequency-doubled femtosecond Er-doped fiber laser

The designed femtosecond fiber laser consists of two stages: an all-fiberized part for the pump light generation up to 2150 nm and a free-space optical part for the SHG tunable from 872 to 1075 nm. The laser source scheme is presented in Fig. 1.

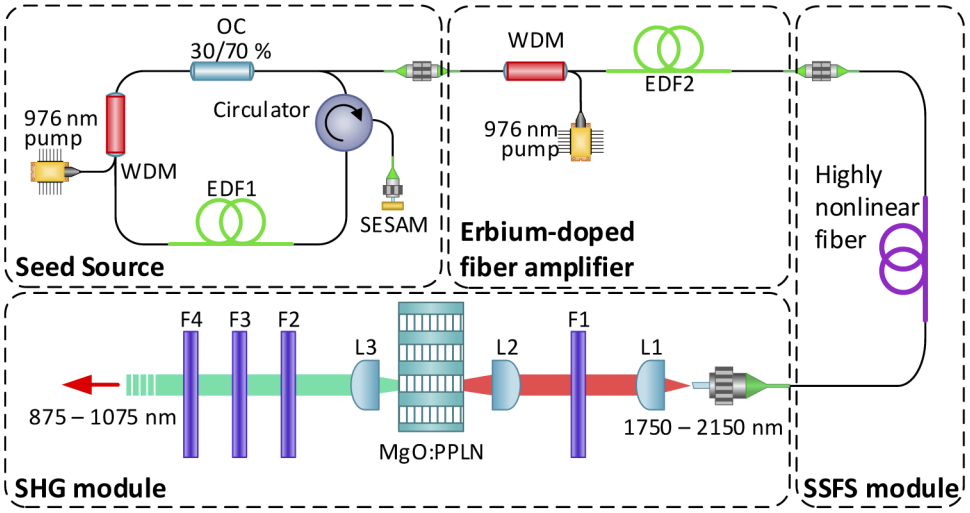

Fig. 1. Scheme of the spectrally shifted, frequency-doubled fiber laser source: EDF1, EDF2 - erbium-doped fibers, OC – 70/30% output coupler, WDM – 980/1550 nm wavelength division multiplexer (filter type), SESAM – semiconductor saturable absorber mirror, F1, F2, F3, F4 – spectral filters, L1, L2, L3 – achromatic lenses.

As a seed source, a ring cavity Er-doped fiber laser is used, mode-locked via a semiconductor saturable absorber mirror (SESAM, Batop GmbH). The oscillator is based on a highly erbium-doped active fiber (Liekki Er80-8/125-PM, EDF1). The seed provides pulses with 330 fs duration at a 51.5 MHz repetition rate with an average power of 4 mW at a 1559.6 nm central wavelength. The pulses are then amplified in an erbium-doped fiber amplifier (EDFA) based on a 1.2 m long highly erbium-doped fiber (Liekki Er80-4/125-PM, EDF2). The amplifier was designed to obtain sub-100 fs pulses at its output at the maximum available pumping power (~ 1 W), as explained in our previous work [18]. Amplified pulses were then delivered to the anomalous-dispersion highly nonlinear fiber (HNLF, Fibrain) for SSFS. In the SSFS process, the input pulses are nonlinearly converted towards longer wavelengths via stimulated Raman scattering [21]. Consequently, ultrashort pulses with central wavelengths tunable from 1742 to 2136 nm were obtained. The broad spectral tuning of the shifted solitons is possible by tuning the optical power coupled into the HNLF only, i.e., by controlling the pump power of the erbium-doped fiber amplifier. The HNLF was spliced with a PM-SMF fiber at its input and output with less than 0.8 dB loss per splice, and connected to the amplifier's output via FC/APC fiber connector. Measured optical spectra of seventeen solitons, the corresponding pulse autocorrelations, and the average power vs. wavelength characteristics are presented in Supplement 1, Figures S1 and S2 (section A). Within the tuning range, the average power increases from approx. 6 mW for the shorter wavelengths to

Biomedical Optics EXPRESS

more than 20 mW for longer ones. For the two longest central-wavelength solitons (2111 nm and 2136 nm), the average power decreases slightly due to the appearance of the higher-order soliton; however, the unwanted spectral components are filtered out in the SHG module. The entire setup is based only on polarization-maintaining (PM) fibers and components, ensuring linear polarization with excellent stability, crucial for the SHG process.

Subsequently, the soliton pulses were frequency-doubled in an SHG module shown in Fig. 1. The output of the HNLF was collimated using an achromatic lens L1 (10 mm focal length, AC-080-010-C-ML, Thorlabs). Then we applied a long-pass filter F1, with the 1500 nm cut-on wavelength (FELH1500, Thorlabs) to block unwanted light below 1.5 µm. The collimated beam was then focused by an achromatic lens L2 (16 mm focal length, AC-080-016-C-ML, Thorlabs) on a MgO:PPLN crystal (HC Photonics Corp.) with 17 quasi-phase matching (QPM) periods (24.5–32.5 µm) and a poling length of 5 mm. The 5 mm poling length was intentionally chosen to limit the spectral width of the SHG signal, essential for the application of the system in the 2PV measurement. The SHG module enables laser beam coupling to each of the 17 QPM channels of the crystal by moving it perpendicular to the beam direction using a manual linear stage with about 12 mm travel. Position of each period was determined experimentally and its repeatability was sufficient to choose desired period at any moment, allowing for convenient tuning of the wavelength. Then, the generated second harmonic signal beam was collimated using an achromatic lens L3 (25 mm focal length, AC127-025-B-ML, Thorlabs). Unwanted wavelengths were removed with the set of three filters: shortpass 1150 nm (F2) transmitting signal within 535–1135 nm range (Edmund Optics), shortpass 1600 nm (F3) transmitting the signal in the 810–1540 nm range (Edmund Optics), and longpass filter with the cut-on wavelength of 800 nm F4 (FELH 800, Thorlabs). The F2 and F3 filters effectively attenuate the residual pump signal of 1.56–2.14 µm, while the F4 filter attenuates unwanted higher harmonics below 800 nm generated in the PPLN crystal. All filters used in this setup were chosen to make the output signal safe for work with a human eye [29].

3. Characterization of the laser output parameters

Figure 2 presents normalized SHG spectra together with average power and pulse duration

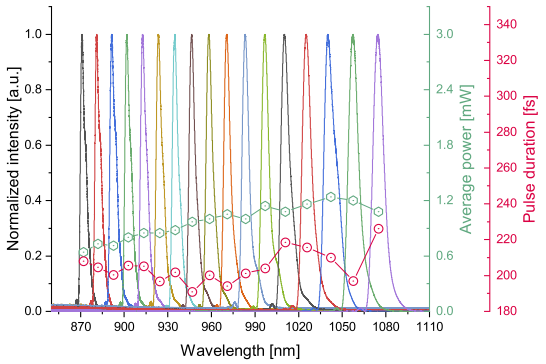

Fig. 2. Generated second harmonic spectra with measured pulse duration and average power in the 200-nm spectral range.

for each of the seventeen PPLN periods. The pulse duration varies slightly from 191 to 226 fs, which is sufficiently even and safe for the needs of a 2PV application. The output power ranges from 0.68 to 1.24 mW, corresponding to pulse energy between 13.2 and 24.1 pJ. Longer wavelengths tend to have higher power which is related to the increased input power delivered to the HNLF fiber, allowing for spectral tuning towards longer wavelengths. The recorded full

Biomedical Optics EXPRESS

width at half-maximum (FWHM) of optical spectra increases from 4.5 to 9.9 nm with increasing central wavelength.

The temporal and spectral intensities, measured via the frequency-resolved optical gating technique (Mesa Photonics FS-Ultra2, FROG) for five chosen wavelengths covering the 200 nm tuning range (872.1 nm, 913.6 nm, 958.8 nm, 1011.0 nm, and 1074.9 nm) are presented in Fig. 3. The pulse duration is sufficiently constant, and its mean value is 205 fs (with standard deviation = 9 fs). The recorded temporal and spectral intensity profiles for all seventeen operating central wavelengths are presented in the Supplement 1, Fig. S3 (section A).

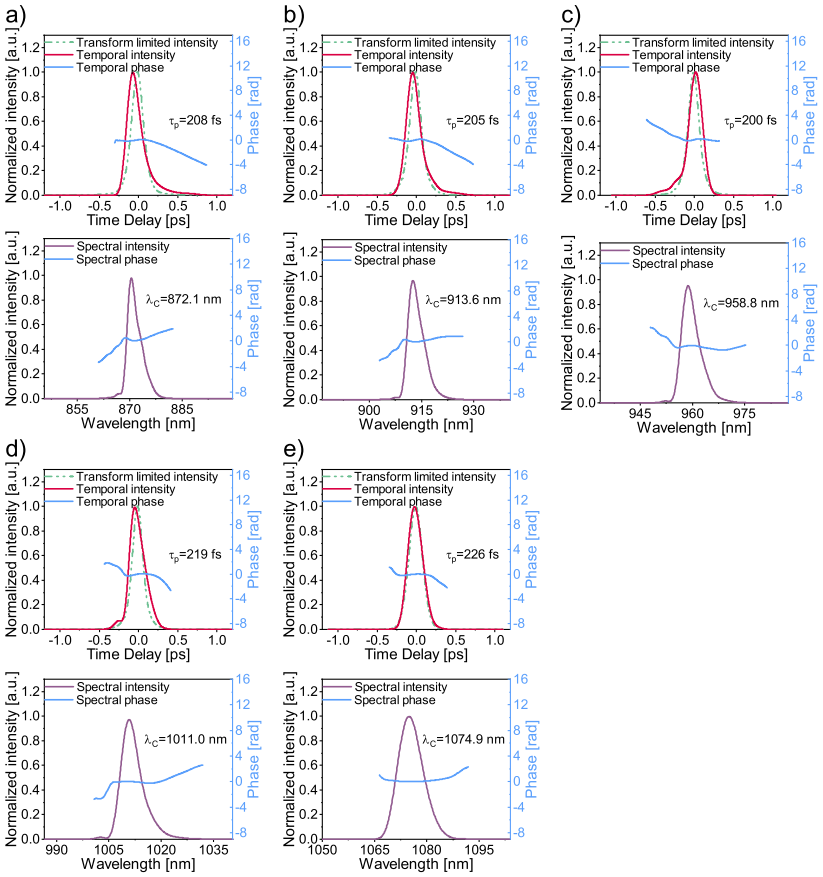

Fig. 3. Recorded FROG temporal intensities for the pulses (solid red line, up) and corresponding spectral intensities (solid purple line, down) for central wavelengths of: (a) 872.1 nm, (b) 913.6 nm, (c) 958.8 nm, (d) 1011.0 nm and (e) 1074.9 nm together with the temporal and spectral phase (solid blue line).

The measured and retrieved FROG spectrograms for the same operating central wavelengths as in Fig. 3 are presented in Fig. 4. The recorded FROG spectrograms for the seventeen operating central wavelengths are presented in the Supplement 1, Fig. S4 (section A). The FROG measurement revealed a clean pulse shape without any pronounced sidebands and a nearly flat temporal phase.

Figure 5 presents the average power stability measured over 4 hours for five central wavelengths (same as in Fig. 3 and Fig. 4) covering the 200 nm tuning range. The system has an excellent power stability of 0.03% rms in the best case for the 958.8 nm wavelength and 0.15% rms in the worst case for the 872.1 nm wavelength, which is decent, considering that the fiberized part of

Biomedical Optics EXPRESS

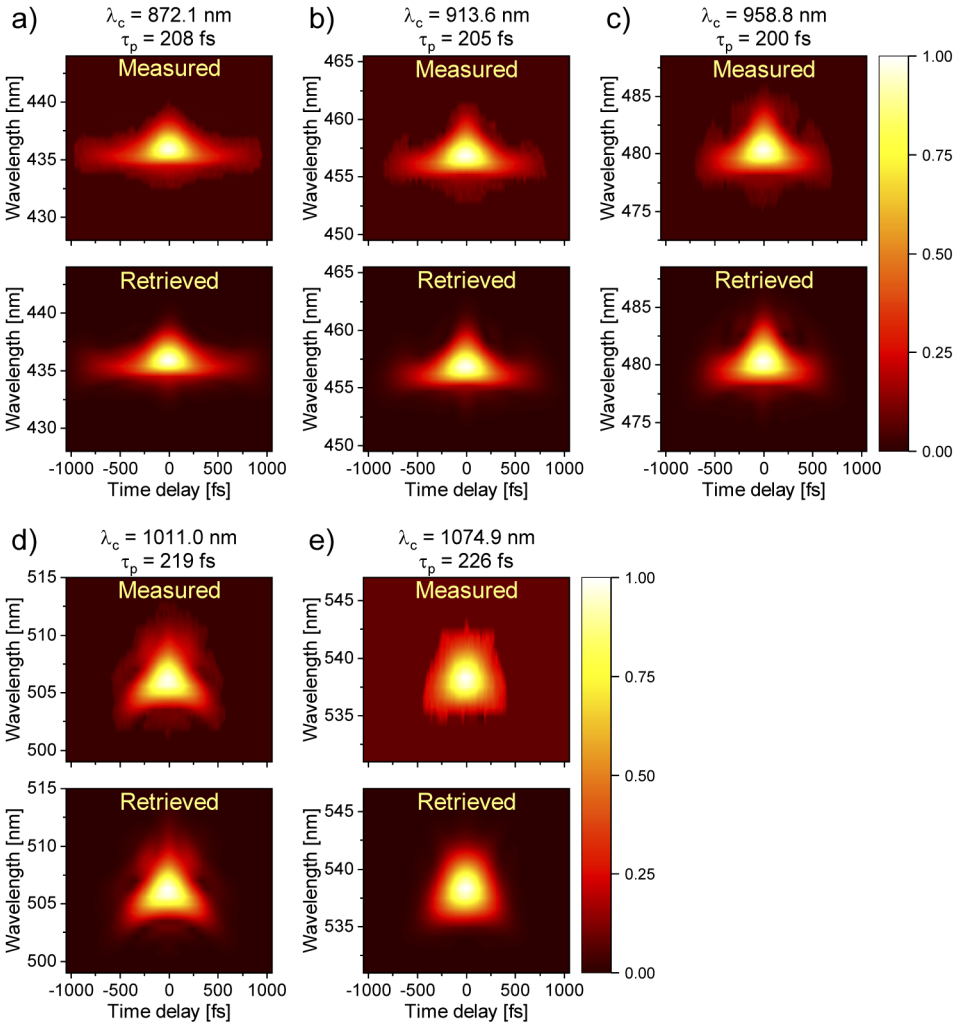

Fig. 4. Measured and retrieved FROG spectrograms for (a) 872.1 nm, (b) 913.6 nm, (c) 958.8 nm, (d) 1011.0 nm, and (e) 1074.9 nm operating central wavelength.

the system was not temperature-stabilized. This long-term measurement confirms that the source provides stable, consistent optical power during a human eye examination, typically lasting up to several minutes.

The pulse parameters for the seventeen operating central wavelengths (17 PPLN periods), such as full width at half maximum (FWHM), pulse duration, average power, and pulse energy, are summarized in the Supplement 1, Table S1 (section A).

Biomedical Optics EXPRESS

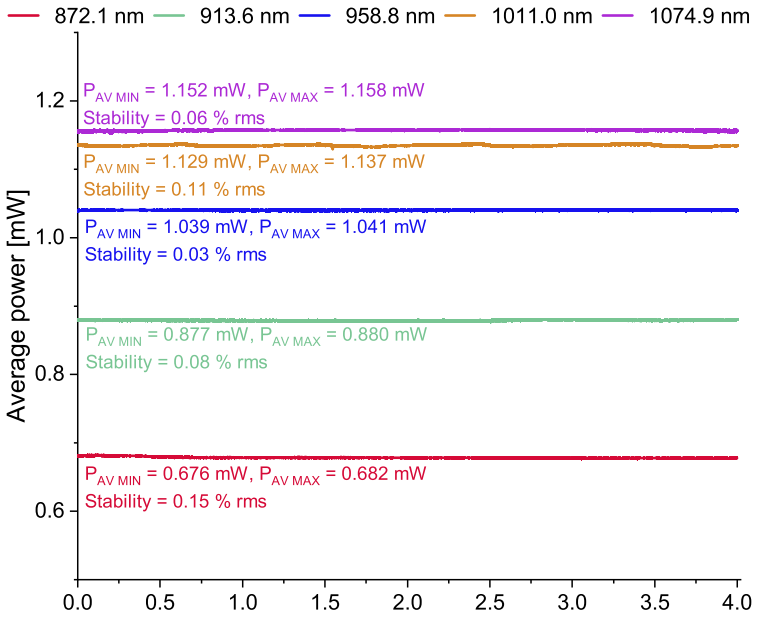

Fig. 5. Long-term average power stability measurement over a period of 4 hours measured for operating central wavelengths of 872.1 nm, 913.6 nm, 958.8 nm, 1011.0 nm, and 1074.9 nm.

4. Application of the laser system developed for the two-photon vision investigations

The laser described in the previous chapter was subsequently applied for 2PV studies. In this regard, we have integrated the laser presented above with our optical setup shown in Fig. 6. First, the laser beam was directed through a neutral density filter F in order to attenuate it to the safety limits and two long-pass filters – F1 and F2 (FELH0850, Thorlabs), with a cutoff wavelength of 850 nm to filter any visible radiation (attenuation greater than 10 folds of magnitude). We have used a gradient filter GF (NDC-50C-4, Thorlabs, variable optical density from 0 to 4.0) steered by a stepper motor SM (ST4209X1004-A, Nanotec, 1/64 step operating mode) to adjust the brightness of the stimulus, which was additionally constantly monitored after the telescope L1-L2 during tests with the power meter (S120C, Thorlabs). The telescope consisted of L1 and L2 lenses, with 150 mm (wavelengths up to 1027 nm) or 75 mm (for 1042 nm and longer wavelengths) and 150 mm focal lengths, respectively. The lens L1 was changed to keep approximately the same beam size at the eye's pupil plane for the whole tuning range. After the telescope L1-L2, the laser beam was shaped into a 0.5 deg (Goldmann size III) flickering circle stimulus using galvanometric scanners GSC (GVS002, Thorlabs) and displayed onto the subjects' retina at the specified location (in this case, fovea center). The laser beam diameter ($1/e^2$) at eye's pupil was approximately 1.0×1.2 mm. Additionally, a fixation point (visible red light, 630 nm wavelength) was used to support the subject in maintaining the eye in a stable position. Correction of the subject's eye refraction for the stimulus and fixation point was provided by moving lenses L3 and L6. The subject's eye was illuminated using a pupil illuminator ($\lambda = 850$ nm, 30 nm FWHM bandwidth), allowing constant monitoring of the subjects' pupil position during the test with a monochrome pupil camera (DCC1545M, Thorlabs); bandpass filter (BPF) placed in front of the camera transmitted only the illuminator wavelength. The system is described in detail in our previous work [8].

By applying the so-called method of adjustment [30], we have measured the visual threshold in the entire available spectral range for three healthy, dark-adapted experienced subjects (one

Biomedical Optics EXPRESS

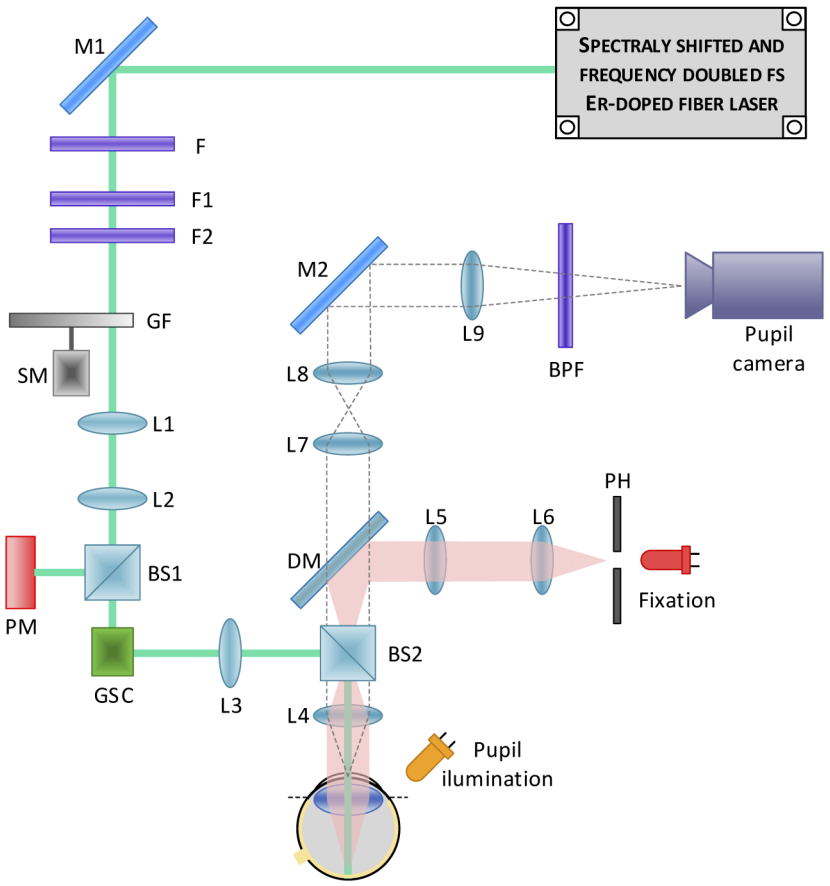

Fig. 6. Optical system used to measure the scotopic luminance curve in two-photon vision. Symbols: M – mirror, F – neutral density filter, GF – neutral density gradient filter, SM – stepper motor, BS – beam splitter (BS1 – 10R:90 T, BS2 – 90R:10 T), PM – power monitor, GSC – galvanometric scanners, DM – dichroic mirror, PH – pinhole, BPF – bandpass filter, L – lens. Focal lengths of achromatic lenses (B-coated): L1 – 150 mm (PPLN periods 1-14)/75 mm (PPLN periods 15-17), L2 – 150 mm, L3 – 100 mm, L4 – 50 mm, L5 – 75 mm, L6 – 50 mm, L7 – 75 mm, L8 – 200 mm, L9 – 25 mm.

female, two male). For each wavelength, five visual threshold measurements were made during a single test, which lasted 1 to 3 minutes. We calculated the final visual threshold as a geometrical mean of two independent measurements: when the stimulus changed brightness from seen to unseen and in the opposite direction. As previously reported [9,31], in the range of 870–940 nm, the stimulus was perceived as red close to the absolute threshold of vision and as a mixture of red and blue for higher intensities. For these wavelengths, the two-photon visual threshold was found as a disappearance/appearance of the blue-colored sensation. Additionally, the absolute subject's visual thresholds measured for these wavelengths, i.e., disappearance/appearance of red color sensation, indicate the one-photon threshold of vision. The red-colored perception was not present for wavelengths 947 nm and longer stimuli. For these wavelengths, the absolute threshold of vision is indicated as the two-photon visual threshold. The wavelength 947 nm was perceived as blue and the longer ones as greenish-blue to green. The average beam power at pupil plane for each wavelength was kept below ANSI limits [29] calculated for multiple pulse exposure lasting for 30 minutes for immobilized eye and stationary spot – this safety level is also shown in

Biomedical Optics EXPRESS

Fig. 7 as a solid red line. The detailed calculations of safety limits are provided in Supplement 1, section B. All tests were performed after obtaining written informed consent. All procedures complied with the Declaration of Helsinki and were approved by the Ethics Committee of the Collegium Medicum, NCU.

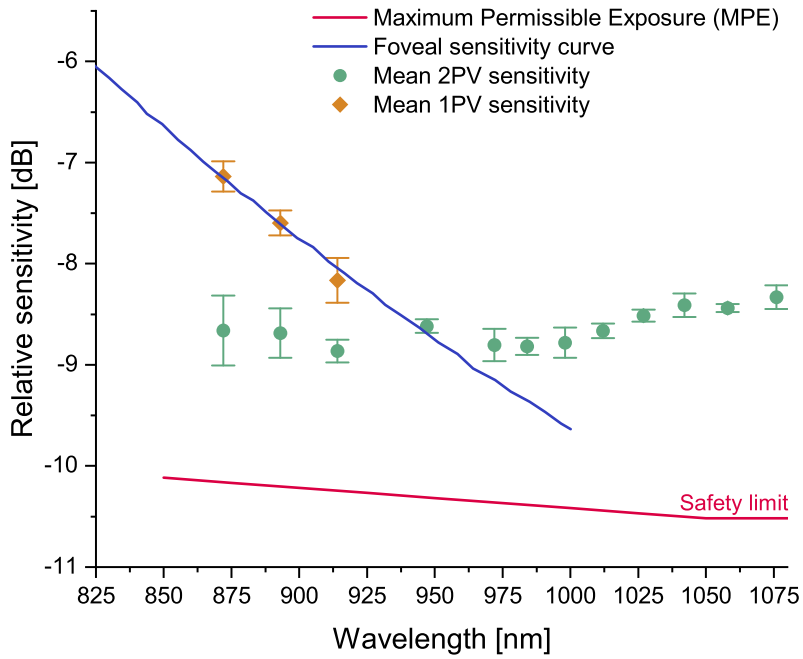

Fig. 7. Measurement data of two-photon vision sensitivity values related to the foveal sensitivity curve [32]. Dots represent mean values, while error bars represent one standard deviation. The red line is based on safety calculations for exposure of immobilized eye for stationary beam lasting 30 min, discussed in section B of supplement.

All visual threshold data were normalized to refer to the classic one-photon foveal sensitivity curve in the near-infrared region [32] and recalculated to the relative sensitivity (*Sens*) value using the following formula:

$$Sens = \log \frac{16.2\ \text{fW}}{P_{Threshold}},$$

where $P_{Threshold}$ is the measured power level at the threshold of vision, and 16.2 fW is a power level corresponding to the threshold of vision at 505 nm, which is the peak of the foveal sensitivity curve [32].

In Fig. 7, sensitivity mean values and standard deviations calculated from all the subjects' answers (5 values for each of the 3 subjects) for each wavelength and vision mechanism (one- and two-photon vision) are presented. It can be seen that measured two-photon sensitivity slightly increases as a function of the wavelength, and all values are significantly above the maximum permitted exposure levels specified in the ANSI standard. In other words, the power level at the threshold of vision is significantly lower than the maximum permitted exposure, determined based on the ANSI standard. The visual thresholds for one- and 2PV in the case of the first three wavelengths were easily determined and measured. For these wavelengths, the error bars for two-photon thresholds are relatively smaller than in [9], which may indicate that two-photon stimulation in the case of our laser was more efficient than for supercontinuum of 1 ns pulses and repetition rate at the order of 10 kHz used by Manzanera et al. [9].

Biomedical Optics EXPRESS

The efficiency of the two-photon vision process depends on the integrated, over time, instantaneous power squared, as shown in our previous work [8]. This approach enables us to compare this process for pulsed lasers emitting radiation at the same wavelength but having various pulse duration and/or pulse repetition rates. We checked that the threshold values obtained for the 1042 nm wavelength (PPLN period no. 14) agree with the previously obtained data for laser pulse trains at similar wavelengths and different pulse train parameters, taking into account the influence of pulse duration and repetition rate [8,10].

The results shown here were obtained with a sufficient number of measurement points in the spectral region above 950 nm, where the 2PV effect dominates, contrary to [5,9]. The adopted measurement protocol also allows us to conclude that the two-photon sensitivity curve reported by Dmitriev et al. was corrupted by a systematic error (probably optical interference in the system). Furthermore, the pulse length and repetition frequency of the constructed laser allows for very efficient and safe two-photon stimulation of the human visual system, as proved by the good separation between one- and two-photon thresholds for wavelengths below 950 nm. The constructed laser may be used for two-photon stimulation of S-cones with 950 nm wavelength without simultaneous stimulation of L-cones by a one-photon process as proved by blue color perception for that wavelength without the addition of red. The future improvements of the laser can further increase the efficiency of two-photon stimulation by reducing the repetition rate, allowing higher peak power for the same average power of the pulse train while still maintaining within the safety regime for the eye [33]. Such an approach allowed us to increase the two-photon excited fluorescence signal in our previous studies [18].

5. Summary

In conclusion, we reported a compact and simple system for efficient 2PV investigation. The system was based on the Er-doped femtosecond fiber laser, which is spectrally shifted and frequency-doubled, providing a wide spectral operating range of about 200 nm, ranging from 872 to 1075 nm. The sub-230 fs pulse duration, nearly constant in the entire spectral tuning range, enabled reliable and safe 2PV measurements, providing comprehensive data. The developed system allowed us to reliably describe the scotopic luminosity curve for 2PV for 3 healthy subjects, showing auspicious preliminary results. In addition, our laser system can be an excellent and unique tool for diagnosing ocular pathology or for monitoring treatment. The average output power of the system (between 0.68 and 1.24 mW) was fully sufficient and safe for the presented 2PV measurement in the human eye.

Funding. Fundacja na rzecz Nauki Polskiej (First TEAM/2017-4/39, MAB/2019/12, TEAM TECH/2016-3/20); Narodowe Centrum Nauki (2016/23/B/ST2/00752).

Acknowledgments. The International Centre for Translational Eye Research (MAB/2019/12) project is carried out within the International Research Agendas programme of the Foundation for Polish Science co-financed by the European Union under the European Regional Development Fund. First TEAM and TEAM TECH projects are funded by the Foundation for Polish Science cofinanced by the European Union under the European Regional Development Fund. KK acknowledges the National Science Centre.

Disclosures. The authors declare no conflicts of interest.

Data availability. Data underlying the results presented in this paper are available from the authors upon request.

Supplemental document. See Supplement 1 for supporting content.

References

1. E. E. Hoover and J. A. Squier, "Advances in multiphoton microscopy technology," Nat. Photonics **7**(2), 93–101 (2013).
2. Y. Ozeki, W. Umemura, Y. Otsuka, S. Satoh, H. Hashimoto, K. Sumimura, N. Nishizawa, K. Fukui, and K. Itoh, "High-speed molecular spectral imaging of tissue with stimulated Raman scattering," Nat. Photonics **6**(12), 845–851 (2012).
3. W. Denk, J. H. Strickler, and W. W. Webb, "Two-Photon Laser Scanning Fluorescence Microscopy," Science **248**(4951), 73–76 (1990).

Biomedical Optics EXPRESS

4. D. Ruminski, G. Palczewska, M. Nowakowski, A. Zielińska, V. J. Kefalov, K. Komar, K. Palczewski, and M. Wojtkowski, "Two-photon microperimetry: sensitivity of human photoreceptors to infrared light," Biomed. Opt. Express **10**(9), 4551–4567 (2019).
5. G. Palczewska, F. Vinberg, P. Stremplewski, M. P. Bircher, D. Salom, K. Komar, J. Zhang, M. Cascella, M. Wojtkowski, V. J. Kefalov, and K. Palczewski, "Human infrared vision is triggered by two-photon chromophore isomerization," Proc. Natl. Acad. Sci. U. S. A. **111**(50), E5445–E5454 (2014).
6. F. Vinberg, G. Palczewska, J. Zhang, K. Komar, M. Wojtkowski, V. J. Kefalov, and K. Palczewski, "Sensitivity of Mammalian Cone Photoreceptors to Infrared Light," Neuroscience **416**, 100–108 (2019).
7. P. Artal, S. Manzanera, K. Komar, A. Gambín-Regadera, and M. Wojtkowski, "Visual acuity in two-photon infrared vision," Optica," Optica **4**(12), 1488–1491 (2017).
8. M. J. Marzejon, Ł. Kornaszewski, J. Bogusławski, P. Ciąćka, M. Martynow, G. Palczewska, S. Maćkowski, K. Palczewski, M. Wojtkowski, and K. Komar, "Two-photon microperimetry with picosecond pulses," Biomed. Opt. Express **12**(1), 462–479 (2021).
9. S. Manzanera, D. Sola, N. Khalifa, and P. Artal, "Vision with pulsed infrared light is mediated by nonlinear optical processes," Biomed. Opt. Express **11**(10), 5603–5617 (2020).
10. M. Marzejon, Ł. Kornaszewski, M. Wojtkowski, and K. Komar, "Effects of laser pulse duration in two-photon vision threshold measurements," in *Ophthalmic Technologies XXXI* (SPIE, 2021), Vol. 11623, pp. 74–79.
11. K. Komar, M. J. Marzejon, A. Matuszak, B. Sikorski, and M. Wojtkowski, "The effect of cataract on two-photon visual thresholds," Invest. Ophthalmol. Visual Sci. **62**, 2009 (2021).
12. A. Zielinska, P. Ciacka, M. Szkulmowski, and K. Komar, "Pupillary Light Reflex Induced by Two-Photon Vision," Invest. Ophthalmol. Visual Sci. **62**(15), 23 (2021).
13. V. G. Dmitriev, V. N. Emel'yanov, M. A. Kashintsev, V. V. Kulikov, A. A. Solov'ev, M. F. Stel'makh, and O. B. Cherednichenko, "Nonlinear perception of infrared radiation in the 800–1355 nm range with human eye," Sov. J. Quantum Electron. **9**(4), 475–479 (1979).
14. G. Łabuz, A. Rayamajhi, J. Usinger, K. Komar, P. Merz, R. Khoramnia, G. Palczewska, K. Palczewski, and G. U. Auffarth, "Clinical Application of Infrared-Light Microperimetry in the Assessment of Scotopic-Eye Sensitivity," Trans. Vis. Sci. Tech. **9**(8), 7 (2020).
15. G. Łabuz, A. Rayamajhi, R. Khoramnia, G. Palczewska, K. Palczewski, A. Holschbach, and G. U. Auffarth, "The loss of infrared-light sensitivity of photoreceptor cells measured with two-photon excitation as an indicator of diabetic retinopathy: A Pilot Study," Retina, **41**, 61302–1308 (2020).
16. A. Zielińska, K. Kiluk, M. Wojtkowski, and K. Komar, "System for psychophysical measurements of two-photon vision," Photonics Lett. Pol. **11**(1), 1–3 (2019).
17. J. K. Bowmaker and H. J. Dartnall, "Visual pigments of rods and cones in a human retina," J Physiol **298**(1), 501–511 (1980).
18. D. Stachowiak, J. Bogusławski, A. Głuszek, Z. Łaszczych, M. Wojtkowski, and G. Soboń, "Frequency-doubled femtosecond Er-doped fiber laser for two-photon excited fluorescence imaging," Biomed. Opt. Express **11**(8), 4431–4442 (2020).
19. F. M. Mitschke and L. F. Mollenauer, "Discovery of the soliton self-frequency shift," Opt. Lett. **11**(10), 659–661 (1986).
20. J. Luo, B. Sun, J. Ji, E. L. Tan, Y. Zhang, and X. Yu, "High-efficiency femtosecond Raman soliton generation with a tunable wavelength beyond 2 μm," Opt. Lett. **42**(8), 1568–1571 (2017).
21. N. Nishizawa and T. Goto, "Widely wavelength-tunable ultrashort pulse generation using polarization maintaining optical fibers," IEEE J. Sel. Top. Quantum Electron. **7**(4), 518–524 (2001).
22. J.-Y. Huang, L.-Z. Guo, J.-Z. Wang, T.-C. Li, H.-J. Lee, P.-K. Chiu, L.-H. Peng, and T.-M. Liu, "Fiber-based 1150-nm femtosecond laser source for the minimally invasive harmonic generation microscopy," J. Biomed. Opt. **22**(03), 1 (2017).
23. K. Charan, B. Li, M. Wang, C. P. Lin, and C. Xu, "Fiber-based tunable repetition rate source for deep tissue two-photon fluorescence microscopy," Biomed. Opt. Express **9**(5), 2304–2311 (2018).
24. A. Zach, M. Mohseni, C. Polzer, J. W. Nicholson, and T. Hellerer, "All-fiber widely tunable ultrafast laser source for multimodal imaging in nonlinear microscopy," Opt. Lett. **44**(21), 5218–5221 (2019).
25. B. Li, M. Wang, K. Charan, M. Li, and C. Xu, "Investigation of the long wavelength limit of soliton self-frequency shift in a silica fiber," Opt. Express **26**(15), 19637–19647 (2018).
26. L.-T. Chou, Y.-C. Liu, D.-L. Zhong, W.-Z. Lin, H.-H. Hung, C.-J. Chan, Z.-P. Chen, and S.-H. Chia, "Low noise, self-phase-modulation-enabled femtosecond fiber sources tunable in 740-1236 nm for wide two-photon fluorescence microscopy applications," Biomed. Opt. Express **12**(5), 2888–2901 (2021).
27. K. Wang, T.-M. Liu, J. Wu, N. G. Horton, C. P. Lin, and C. Xu, "Three-color femtosecond source for simultaneous excitation of three fluorescent proteins in two-photon fluorescence microscopy," Biomed. Opt. Express **3**(9), 1972–1977 (2012).
28. G. Krauss, T. Hanke, A. Sell, D. Träutlein, A. Leitenstorfer, R. Selm, M. Winterhalder, and A. Zumbusch, "Compact coherent anti-Stokes Raman scattering microscope based on a picosecond two-color Er:fiber laser system," Opt. Lett. **34**(18), 2847–2849 (2009).
29. . "American National Standard for Safe Use of Lasers ANSI Z136.1.," (2014).
30. C. H. Graham, *Vision and Visual Perception*. Clarence H. Graham , Editor, Wiley(New York, 1965).

Biomedical Optics EXPRESS

31. K. Komar, A. Zielinska, D. Ruminski, M. Marzejon, P. Ciacka, L. Kornaszewski, S. Manzanera, P. Artal, and M. Wojtkowski, "The limits of perception of light by two-photon vision," Invest. Ophthalmol. Vis. Sci. **60**, 3907 (2019).
32. D. R. Griffin, R. Hubbard, and G. Wald, "The Sensitivity of the Human Eye to Infra-Red Radiation," J. Opt. Soc. Am. **37**(7), 546–554 (1947).
33. J. Boguslawski, G. Palczewska, S. Tomczewski, J. Milkiewicz, P. Kasprzycki, D. Stachowiak, K. Komar, M. J. Marzejon, B. L. Sikorski, A. Hudzikowski, A. Głuszek, Z. Łaszczych, K. Karnowski, G. Soboń, K. Palczewski, and M. Wojtkowski, "In vivo imaging of the human eye using a 2-photon-excited fluorescence scanning laser ophthalmoscope," J. Clin. Invest. **132**(2), e154218 (2022).